

The Hydrogen Atomic Model Based on the Electromagnetic Standing Waves and the Periodic Classification of the Elements

Giuseppe Bellotti¹

¹ 14/C, S. Gaudenzio Street, 10015 Ivrea (To), Italy

Correspondence: Giuseppe Bellotti, 14/C, S. Gaudenzio Street, 10015 Ivrea (To), Italy. E-mail: giuseppe.bellotti@live.it

Received: June 19, 2012 Accepted: July 6, 2012 Online Published: July 27, 2012

doi:10.5539/apr.v4n3p141

URL: <http://dx.doi.org/10.5539/apr.v4n3p141>

Abstract

By means of a new concept of the Hydrogen atomic structure [where the electron of the Hydrogen is considered not as a non-dimensional object revolving around the atomic nucleus in a field of central forces, but as a three-dimensional electromagnetic spherical standing wave concentrically superimposed on the electromagnetic standing wave of the proton] we can obtain a new periodic classification of the elements. Up till now, chemistry has considered atoms to be made up of sub-shells with 2, 6, 10, 14 electrons and currently, the great number of electrons (14) in sub-shells f creates some problems in the formation of the sixth and seventh periods. Instead in this paper we will only consider sub-shells with 2, 6, 10 electrons, to achieve a better ordering of the heavy metals. Hence, Ni, Pd, and Yb have been drawn up in columns in the new periodic classification of elements, and Ytterbium could be proposed as a testing material in the cold fusion experiments. Moreover many new theoretical (albeit unsteady) electromagnetic wave-lengths of Hydrogen Spectrum appear.

Keywords: periodic classification of elements, hydrogen atomic model, electromagnetic standing waves, hydrogen spectrum

1. Introduction

A new concept of the Hydrogen atomic structure (where the Hydrogen electron is considered not as a non-dimensional object revolving around the atomic nucleus in a field of central forces, but as a three-dimensional electromagnetic (e.m.) spherical standing wave concentrically superimposed on the e.m. standing wave of the proton) has been previously considered in (Bellotti, 2011).

Since the e.m. standing waves have a defined angular frequency ω_γ , then the wave equation can be written as:

$$c^2 \nabla^2 \psi = \frac{\partial^2 \psi}{\partial t^2} = -\omega_\gamma^2 \psi \quad (1)$$

where:

$$\psi(r, \vartheta, \varphi, t) = R(r)\Theta(\vartheta)\Phi(\varphi)T(t) \quad (2)$$

ψ is a function defined in polar coordinates (r, θ, φ); t is time and c is the speed of light.

In (Bellotti, 2011) the following results were demonstrated:

$$E = \frac{h}{2\pi} \omega_\gamma \propto k^2 \quad (3)$$

Where: E is the energy of the e.m. standing wave; ω_γ is the angular frequency of the e.m. standing wave and $k = \frac{\pi}{a_0}$ is wave number; a_0 is the radius of the first nodal surface of the electron, considered to be an e.m. spherical standing wave.

$$\Phi(\varphi) = \frac{1}{\sqrt{\pi}} \sin\left(m\varphi + \frac{\pi}{4}\right) \quad (4)$$

where $m \in \mathbb{Z}$ is the magnetic quantum number.

The functions $\Theta(\theta)$ are :

$$\begin{aligned}\Theta(x = \cos(\vartheta)) = P_l(x) &= \frac{1}{2^l l!} \frac{d^l}{dx^l} (x^2 - 1)^l && \text{for } m = 0 \\ \Theta(x) = P_l^m(x) &= (1 - x^2)^{\frac{|m|}{2}} \frac{d^{|m|}}{dx^{|m|}} (P_l(x)) && \text{for } m \neq 0\end{aligned}\quad (5)$$

The equations in 5 are not normalized. They can be normalized as per (Persico 1971).

$$T(t) = K \sin(\omega_p t + G) \quad (6)$$

Where: K = the amplitude G = the phase

$$\begin{aligned}R_0(r) &= \frac{1}{r} \{ [\sin(kr)] + A_0 [\cos(kr)] \} \\ R_1(r) &= \frac{1}{r} \left\{ \left[\sin(kr) + \frac{\cos(kr)}{kr} \right] + A_1 \left[\cos(kr) - \frac{\sin(kr)}{kr} \right] \right\} \\ R_2(r) &= \frac{1}{r} \left\{ \left[\sin(kr) + \frac{3\cos(kr)}{kr} - \frac{3\sin(kr)}{(kr)^2} \right] + A_2 \left[\cos(kr) - \frac{3\sin(kr)}{kr} - \frac{3\cos(kr)}{(kr)^2} \right] \right\} \\ R_3(r) &= \frac{1}{r} \left\{ \left[\sin(kr) + \frac{6\cos(kr)}{kr} - \frac{15\sin(kr)}{(kr)^2} - \frac{15\cos(kr)}{(kr)^3} \right] + \right. \\ &\quad \left. + A_3 \left[\cos(kr) - \frac{6\sin(kr)}{kr} - \frac{15\cos(kr)}{(kr)^2} + \frac{15\sin(kr)}{(kr)^3} \right] \right\} \\ R_4(r) &= \frac{1}{r} \left\{ \left[\sin(kr) + \frac{10\cos(kr)}{kr} - \frac{45\sin(kr)}{(kr)^2} - \frac{105\cos(kr)}{(kr)^3} + \frac{105\sin(kr)}{(kr)^4} \right] + \right. \\ &\quad \left. + A_4 \left[\cos(kr) - \frac{10\sin(kr)}{kr} - \frac{45\cos(kr)}{(kr)^2} + \frac{105\sin(kr)}{(kr)^3} + \frac{105\cos(kr)}{(kr)^4} \right] \right\}\end{aligned}\quad (7)$$

with the following values of A_l (where $l = 0, 1, 2, 3, 4$)

$$\begin{aligned}A_0 &= 0 & A_1 &= -\frac{1}{\pi} = -0.318\ 309\ 89 & A_2 &= -\frac{3\pi}{[\pi^2 - 3]} = -1.371\ 953\ 52 \\ A_3 &= \frac{3[2\pi^2 - 5]}{[\pi(15 - \pi^2)]} = 2.743\ 435\ 15 & A_4 &= \frac{5\pi[21 - 2\pi^2]}{\pi^4 - 45\pi^2 + 105} = -0.081\ 930\ 363\end{aligned}\quad (8)$$

We can verify that for $l = 0$ the $R_0(r)$ equation meets the boundary condition $a_0 R_0(a_0) = 0$ even when the wave number $k = \left(\frac{\pi}{a_0}\right)$ is substituted by the wave numbers $k^* = j\left(\frac{\pi}{a_0}\right)$ with $j \in \mathbb{N}$. The corresponding graphs show that each $a_{0,j} = ja_0$ root of $R_0(r)$ is shifted to $r = a_0$ and we have $n = j$ nodal spherical surfaces in the radial interval $[0, a_0]$.

2. The Periodic Classification of the Elements

Using the symbol n_s the sub-shells s joined to the principal quantum number n can be defined. For every sub-shell n_s correspond the functions $R_0(jr) = \frac{1}{r} \sin\left(j\frac{\pi}{a_0}r\right)$ that vanish for $r = a_0$ and that affirm the condition $j = n$. Then the

eigenvector $R_0(r)$ of the 1s sub-shell ($j=1$) shows one nodal surface within the interval of r $[0, a_0]$ (at $r = a_0$); the eigenvector $R_0(2r)$ of 2s sub-shell ($j = 2$) shows two nodal surfaces within $[0, a_0]$; the eigenvector $R_0(3r)$ of 3s sub-shell ($j = 3$), three; and so on. If we establish $a_{0,j}$ to be the j th-root of the function $R_0(r)$ shown in equation 7, then, from (3) and for the ns sub-shells, we can confirm that:

$$E_{0,j} \propto k^2 = \left(\frac{\pi}{a_0}\right)^2 \propto \left(j \frac{\pi}{a_0}\right)^2 \propto j^2 \propto (ja_0)^2 = a_{0,j}^2 \quad j = 1, 2, 3, 4, \dots \quad (9)$$

and, according to equation 21 of (Bellotti, 2009), the total sub-shell energy $E_{l,j}$ that corresponds to each j th-root $a_{l,j}$ of the $R_l(r)$ shown in (7) is:

$$E_{l,j} \propto a_{l,j}^2 \quad (10)$$

If all the w_l eigenvectors of a given (l, j) sub-shell have the same energy $E_{l,j}^*$, then from (10) we have:

$$E_{l,j}^* = \frac{E_{l,j}}{w_l} \propto \frac{a_{l,j}^2}{w_l} \Leftrightarrow \sqrt{E_{l,j}^*} \propto \frac{a_{l,j}}{\sqrt{w_l}} \quad (11)$$

$$\begin{aligned} l = 0 \quad m = 0 &\Rightarrow w_0 = 1 && \text{sub-shells s} \\ l = 1 \quad m = 0, \pm 1 &\Rightarrow w_1 = 3 && \text{sub-shells p} \\ \text{with: } l = 2 \quad m = 0, \pm 1, \pm 2 &\Rightarrow w_2 = 5 && \text{sub-shells d} \\ l = 3 \quad m = 0, \pm 1, \pm 2, \pm 3 &\Rightarrow w_3 = 7 && \text{sub-shells f} \\ l = 4 \quad m = 0, \pm 1, \pm 2, \pm 3, \pm 4 &\Rightarrow w_4 = 9 && \text{sub-shells g} \end{aligned} \quad (12)$$

Where w_l (with $l = 0, 1, 2, 3, \dots$) are the number of equations present in the sub-shells l .

Now by substituting the function $(\sqrt{w_l}r)$ in place of r , within the $R_l(r)$ shown in (7), we obtain the functions $R_l^*(\sqrt{w_l}r)$. The roots $a_{l,j}$ of these functions $R_l^*(\sqrt{w_l}r)$ will be proportional to the square root of the energy $E_{l,j}^*$ of each eigenvector $R_l(jr)$ that has j roots (or sometimes $j-1$ roots, for f and g sub-shells) within the interval of r $[0, a_0]$. The eigenvectors $R_l(jr)$ are calculated by substituting $k^* = j\pi/a_0$ into the equations 7 instead of $k = \pi/a_0$; and by imposing the boundary condition $a_0 R_l(ja_0) = 0$ in order to calculate the corresponding A_l values. Then we can to draw the $R_l^*(\sqrt{w_l}r)$ functions and obtain the graph shown in Figure 1 where the energies $E_{l,j}^*$ of the sub-shells increase in accordance with the following sequence (13):

$$1s (j=1), 1p (j=2), 1d (j=3), 1p^2 (j=3), 1s^2 (j=2), 1f (j=5), 1g (j=6), \dots \quad (13)$$

Thus, each shell associated to the principal quantum number n is formed by the sequence of the sub-shells ns, np, nd, np², ns², nf, ...; where ns, np, nd ... are the first useful root of the functions $R_0^*(\sqrt{w_0}r), R_1^*(\sqrt{w_1}r), \dots$, that belong to the same shell of the principal quantum number n . ns², np², etc., are the second useful root of $R_0^*(\sqrt{w_0}r), R_1^*(\sqrt{w_1}r), \dots$, that belong to the same shell of the principal quantum number n . The root of the type 1d² ($j = 4$), between 1p² and 1s² in Figure 1 is to be omitted since the sub-shell with minimal energy where there are four nodal surfaces within the interval $[0, a_0]$ has to be the sub-shell 1f. Since the eigenvector $R_3(jr)$ of the sub-shell 1f shows four nodal surfaces within the interval $[0, a_0]$ only when $j=5$, then we have to consider the fifth root of $R_3^*(\sqrt{w_3}r)$, whose associated eigenvector is $R_3(5r)$. Now, sub-shell 1f has an energy greater than the energy of sub-shell 1s²; then also sub-shell 1d² must have an energy greater than the energy of sub-shell 1s². Hence, the fourth root of function $R_2^*(\sqrt{w_2}r)$ does not have any corresponding energy value.

In accordance with the fractals form of the superposition of the e.m. standing waves (Bellotti 2011, 370), we presume a filling up of each shell relative to the principal quantum numbers $n = 1, 2, 3, \dots$ in accordance with sub-shell sequence (13) and in order to generate Table 1. In Table 1 there are only the s, p, d sub-shells. Therefore, we have to draw a graph (Figure 2) in order that the sub-shells in Table 1 and the roots of the functions $R_l^*(\sqrt{w_l}r)$ correspond to each other. Now, if we consider the number j of nodal surfaces of the functions $R_l(jr)$ (with $l = 0, 1, 2$) within the interval of r $[0, a_0]$, then this number j also identifies the position of the j th-root $a_{l,j}$ of the corresponding $R_l^*(\sqrt{w_l}r)$.

Table 1. First approach to the periodic classification of the elements

Principal quantum number	Sub-shells coherent with the filling uporder (13)
n = 1	l = 0 1s
n = 2	l = 0 2s
	l = 1 2p
n = 3	l = 0 3s
	l = 1 3p
	l = 2 3d
n = 4	l = 0 4s
	l = 1 4p
	l = 2 4d
	l = 1 4p ²
n = 5	l = 0 5s
	l = 1 5p
	l = 2 5d
	l = 1 5p ²
	l = 0 5s ²
n = 6	l = 0 6s
	l = 1 6p
	l = 2 6d
	l = 1 6p ²
	l = 0 6s ²
n = 7	l = 0 7s
	l = 1 7p

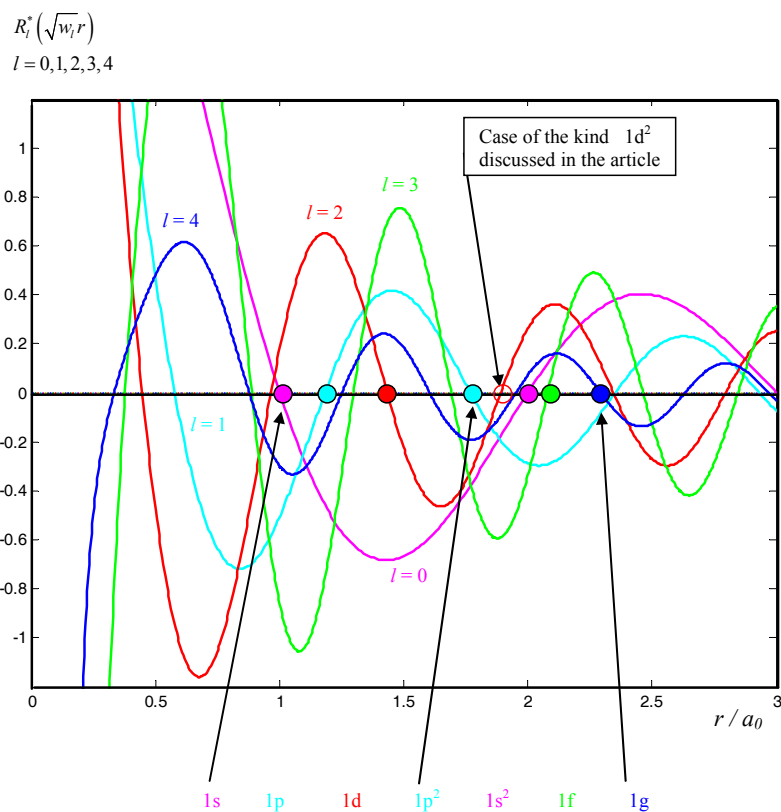


Figure 1. With this graph it is possible to recognize the sequence of sub-shells with increasing energy, valid for each shell that corresponds to the principal quantum number n

Given that the number of roots within the interval $[0, a_0]$ for each eigenvector $R_0(nr)$ of the sub-shell ns is equal to n, we have to consider all the ordered roots $n = 1, 2, 3, \dots$, and 7 of the function $R_0^*(\sqrt{w_0}r)$. The eighth root of $R_0^*(\sqrt{w_0}r)$ will be the sub-shell $5s^2$, the ninth the sub-shell $6s^2$. On the other hand, for each shell related to the principal quantum number n, the number of roots of the functions $R_l(jr)$ within the interval $[0, a_0]$ for sub-shell np ($l = 1$) must be equal to $2n$; those for sub-shell nd ($l = 2$) must be equal to $3n$. For sub-shell $5s^2$ we have shown the position of the eighth root that coincides with $8s$; sub-shell $5p^2$ will have five roots more when compared to $5s^2$ (that is 13); sub-shell $4p^2$ will, instead, have 11 roots [in fact the hypothetical sub-shell $4s^2$ (that does not exist) coincides with $7s$ and we have to consider $7 + 4 = 11$ roots for sub-shell $4p^2$]. Sub-shell $6s^2$ coincides with the position $9s$ and so will have 9 roots; instead sub-shell $6p^2$ will have six roots more, namely, 15 roots.

Now it is possible to generate Table 2, where to each j th-root of the functions $R_0^*(\sqrt{w_0}r)$, $R_1^*(\sqrt{w_1}r)$ and $R_2^*(\sqrt{w_2}r)$ corresponds an eigenvector $R_0(jr)$, $R_1(jr)$ and $R_2(jr)$; moreover each eigenvector $R_0(jr)$, $R_1(jr)$ and $R_2(jr)$ within the interval $[0, a_0]$ gives the number j of nodal surfaces indicated (as roots) in Table II, and all these numbers j of roots coincide with the j th-root $a_{l,j}$ position of the functions $R_l^*(\sqrt{w_l}r)$. Now we can order the sub-shells shown in Table 2 according to the increasing energies $E_{l,j}^*$ shown in Figure 2 and begin building Table III. Through tests, we can check that, for Hydrogen atom, the frequencies $\nu_{A,B}$ that correspond to the transitions $B \rightarrow A$ [where the status A is characterized by the angular quantum number l_A and by the j_A position of the considered root of the function $R_{l_A}^*(\sqrt{w_{l_A}}r)$; and status B is characterized by the angular quantum number l_B and by the j_B position of the considered root of the function $R_{l_B}^*(\sqrt{w_{l_B}}r)$] are obtained in the following Formula 14 (White, 1934):

$$\nu_{A,B} = \frac{E_B^* - E_A^*}{h} = R_\infty c \left(\frac{1}{n_A^2} - \frac{1}{n_B^2} \right) = 3.28984(23) \cdot 10^{15} \left(\frac{1}{n_A^2} - \frac{1}{n_B^2} \right) \text{ Hz} \tag{14}$$

where:

$$R_\infty = \text{Rydberg constant} = 1.097\,373\,12(11) \cdot 10^7 \text{ m}^{-1}$$

Table 2. Second approach to the periodic classification of the elements. The j number of roots within the r interval $[0, a_0]$ of the $R_l(jr)$ eigenvector coincides with the j th-root position of the $R_l^*(\sqrt{w_l}r)$ function

Principal quantum number	Sub-shells coherent with the filling up order (13)		
n = 1	$l = 0$	1s	1 root
n = 2	$l = 0$	2s	2 roots
	$l = 1$	2p	4 roots
n = 3	$l = 0$	3s	3 roots
	$l = 1$	3p	6 roots
	$l = 2$	3d	9 roots
n = 4	$l = 0$	4s	4 roots
	$l = 1$	4p	8 roots
	$l = 2$	4d	12 roots
	$l = 1$	4p ²	11 roots
n = 5	$l = 0$	5s	5 roots
	$l = 1$	5p	10 roots
	$l = 2$	5d	15 roots
	$l = 1$	5p ²	13 roots
	$l = 0$	5s ²	8 roots
n = 6	$l = 0$	6s	6 roots
	$l = 1$	6p	12 roots
	$l = 2$	6d	18 roots
	$l = 1$	6p ²	15 roots
	$l = 0$	6s ²	9 roots
n = 7	$l = 0$	7s	7 roots
	$l = 1$	7p	14 roots

$$c = \text{speed of light} = 2.997\,925\,0(10) \cdot 10^8 \text{ m / s}$$

All the values of the Physical constants are taken from (Jordan, 1988).

n_A^2, n_B^2 = numerical data (shown in Table 3) proportional to the square of the corresponding root values of the functions $R_{i_A}^*(\sqrt{w_{i_A}}r)$ and $R_{i_B}^*(\sqrt{w_{i_B}}r)$,

where we have considered the minimum value of $n_A = n_{l=0, j=1} = 1$

Equation (14) is in accordance with the following equation (15), that was obtained from (9), (10) and (11), applied to ns sub-shells ($l = 0$):

$$E_{0,j}^* = \frac{E_{0,j}}{w_0} \propto \frac{k^2}{w_0} \propto \left(\frac{\pi}{a_0}\right)^2 \propto \frac{1}{(ja_0)^2} = \frac{1}{a_{0,j}^2} \propto -\frac{1}{n_{0,j}^2} \quad j = 1, 2, 3, 4, \dots \quad (15)$$

where $n_{0,j}^2$ has the same meaning as n_A^2, n_B^2 in (14), for $l = 0$.

Now we can assume that the sub-shell energy $E_{l,j}^*$, that corresponds to each j th-root $a_{l,j}$ of $R_i^*(\sqrt{w_i}r)$ obtained from (7), is:

$$E_{l,j}^* = \frac{E_{l,j}}{w_l} \propto \frac{1}{a_{l,j}^2} \propto -\frac{1}{n_{l,j}^2} \quad (16)$$

where the $n_{l,j}^2$ in (16) correspond to either the n_A^2 or n_B^2 in (14), according to the (l_A, j_A) or (l_B, j_B) values. Both the n_A^2 or n_B^2 values are proportional to the square of the corresponding root values $a_{l_A, j_A}, a_{l_B, j_B}$ of the functions $R_{i_A}^*(\sqrt{w_{i_A}}r)$ and $R_{i_B}^*(\sqrt{w_{i_B}}r)$.

Now, by putting $n_A^2 = 1$ and $n_B^2 \rightarrow \infty$ into (14), we can calculate the maximum energy $|E_A^*| = R_\infty c h$ that in a $B \rightarrow A$ transition can be emitted as a light spectrum ray; this energy is half the energy $E = \alpha^2 m_e c^2$ of an elementary e.m. standing wave of radius a_0 (Bellotti, 2011). On the other hand this result is also valid for all the s, p, d sub-shells. In fact we can substitute the equivalent energy referred to the last column of Table 3, in place of n_A^2 , in 14; and we can substitute a value tending towards infinity in place of n_B^2 ; and in accordance with (16) (and its marking), we can obtain two possibilities for emitting a light ray for each eigenvector (an e.m. standing wave) that forms each sub-shell. In fact:

$$-E_{l,j}^* = R_\infty c h \frac{1}{n_{l,j}^2} = \frac{1}{2} (\alpha^2 m_e c^2) \frac{1}{n_{l,j}^2} \quad (17)$$

Where: h = Planck constant; α = fine structure constant and m_e = electron mass.

By returning to (12) and the definition of w_l (with $l = 0, 1, 2, 3, \dots$) being the equation number present in each sub-shell l , we can assume that in the sub-shells s ($l = 0$) we have $w_0 = 2$ possibilities of light emissions (and this value of w_0 can replace the number of equations $w_0 = 1$). In a similar way, we can obtain $w_l = 6$ instead of $w_l = 3$ for the sub-shells p ($l = 1$); $w_2 = 10$ for the sub-shells d ($l = 2$); and so on. The energy property of this eigenvector brings to mind the Pauli principle. So the sequence of the sub-shells shown in Table 3 faithfully reproduces the properties of the elements in their periodic classification in a natural way. Now we can build Table 4. Up till now, chemistry has considered atoms to be made up of sub-shells with 2, 6, 10, 14 electrons and, currently, the great number of electrons, 14, in sub-shells f creates some problems in the formation of the sixth and seventh periods. Instead, Table 3 and Table 4 show that we can consider only sub-shells with 2, 6, 10 electrons, to achieve a better ordering of the heavy metals. Hence, Ni, Pd, and Yb have been drawn up in columns in the new periodic classification of elements, and Ytterbium could be proposed as an optimum material for cold fusion.

The last column of Table 3 shows some real numbers. This is in accordance with Milan Perkovic's considerations on equations (100) - (104) of (Perkovic, 2010). It is possible to go deeper into Perkovic's model in (Perkovic, 2002; Perkovic, 2003).

Table 3. Sequence of the sub-shells filling up, according to the increase in energy

Sub-shells	Transitions Number	Atomic Numbers of the Elements in each sub-shell	Elements of the sub-shell	Energy $n_A^2 \propto a_{l,j}^2$ of the $B=\infty \rightarrow A$ Transition
1s	2	$Z = 1 - 2$	H He	1.000000
2s	2	$Z = 3 - 4$	Li Be	4.000000
2p	6	$Z = 5 - 10$	B C N O F Ne	5.530507
3s	2	$Z = 11 - 12$	Na Mg	9.000000
3p	6	$Z = 13 - 18$	Al Si P S Cl Ar	12.32801
4s	2	$Z = 19 - 20$	K Ca	16.00000
3d	10	$Z = 21 - 30$	Sc Ti V Cr Mn Fe Co Ni Cu Zn	17.17438
4p	6	$Z = 31 - 36$	Ga Ge As Se Br Kr	21.79214
5s	2	$Z = 37 - 38$	Rb Sr	25.00000
4d	10	$Z = 39 - 48$	Y Zr Nb Mo Tc Ru Rh Pd Ag Cd	30.13389
5p	6	$Z = 49 - 54$	In Sn Sb Te I Xe	33.92294
6s	2	$Z = 55 - 56$	Cs Ba	36.00000
4p ²	6	$Z = 57 - 62$	La Ce Pr Nd Pm Sm	40.98833
5d	10	$Z = 63 - 72$	Eu Gd Tb Dy Ho Er Tm Yb Lu Hf	46.69335
6p	6	$Z = 73 - 78$	Ta W Re Os Ir Pt	48.72039
7s	2	$Z = 79 - 80$	Au Hg	49.00000
5p ²	6	$Z = 81 - 86$	Tl Pb Bi Po At Rn	57.11912
5s ²	2	$Z = 87 - 88$	Fr Ra	64.00000
7p	6	$Z = 89 - 94$	Ac Th Pa U Np Pu	66.18450
6d	10	$Z = 95 - 104$	Am Cm Bk Cf Es Fm Md No Lw Ku	66.85278
6p ²	6	$Z = 105 - 110$	Ha ...	75.91658
6s ²	2	$Z = 111 - 112$...	81.00000

Table 4. New periodic classification of the elements. It is interesting to notice the blue column-sequence Ni Pd Yb (No) and to consider Ytterbium for cold fusion experiments

H																	He														
Li	Be											B	C	N	O	F	Ne														
Na	Mg											Al	Si	P	S	Cl	Ar														
K	Ca		Sc	Ti	V	Cr	Mn	Fe	Co	Ni	Cu	Zn		Ga	Ge	As	Se	Br	Kr												
Rb	Sr		Y	Zr	Nb	Mo	Tc	Ru	Rh	Pd	Ag	Cd		In	Sn	Sb	Te	I	Xe												
Cs	Ba	La	Ce	Pr	Nd	Pm	Sm	Eu	Gd	Tb	Dy	Ho	Er	Tm	Yb	Lu	Hf	Ta	W	Re	Os	Ir	Pt	Au	Hg	Tl	Pb	Bi	Po	At	Rn
Fr	Ra	Ac	Th	Pa	U	Np	Pu	Am	Cm	Bk	Cf	Es	Fm	Md	No	Lw	Ku	Ha													

3. Calculation of the Spectral Wave Lengths of Hydrogen

Now we can calculate all the wave-lengths of the Hydrogen spectrum by using the following formula (18) of first approximation, derived from (14) (White, 1934):

$$\lambda_{A,B} = \frac{10^{10}}{R_\infty} \left(\frac{n_A^2 n_B^2}{n_B^2 - n_A^2} \right) \tag{18}$$

where: $R_\infty = 1.097\,373\,12(11) \cdot 10^7 \text{ m}^{-1}$.

n_A^2, n_B^2 are the values shown in the last column of Table 3.

They correspond to the $B \rightarrow A$ transition.

Table 5 shows the most important wavelength that could form the Hydrogen spectrum. But in equation (18) a greater number of Hydrogen spectrum rows were computed compared to the fundamental ones obtained in Quantum Mechanics. This result has to be confirmed by means of a dynamic experimental check. In fact, in all induced mechanical vibrations, the contribution of high order eigenvectors vanishes quickly and only the main eigenvectors, that correspond to the spectrum rows joined to $l=0$ (s sub-shells), are present in the stationary state. As in Quantum Mechanics, now the whole values of n_A^2 (see Table 3) correspond to $l = 0$. Hence, we can obtain the normal rows of emission spectrum of Hydrogen by equation (18). On the other hand, spectrum rows joined to $l=1$ (p sub-shells) and to $l=2$ (d sub-shells), that correspond to the non-whole n_A^2 values, are present only in the transient of Hydrogen atoms excitation. But the presence of either a transient or a stationary state can only be justified when it is possible to consider each Hydrogen atom as a continuous function of energy in a space domain; in other words: when each Hydrogen atom can be considered as an e.m. standing wave. And this condition complies to the fundamental hypothesis of this article. Of course this approach allows for the quantization of energy, since the wave equation eigenvectors can take on different discrete values of energy (see Figure 2).

Then it seems that the traditional idea, i.e. the rows of atomic emission spectra are produced by quantum jumps of the electrons between two different energy levels, has to be formulated in a different way.

Table 5. The most important rows of Hydrogen spectrum expressed in nm

6s ² 1s 92.26579		6p ² 1s 92.34309
	6d 1s 92.5105	
7p 1s 92.52469		5s ² 1s 92.57317
	5p ² 1s 92.75052	
7s 1s 93.02518		6p 1s 93.03631
	5d 1s 93.12102	
4p ² 1s 93.40554		6s 1s 93.73034
	5p 1s 93.89459	
4d 1s 94.25456		5s 1s 94.92365
	4p 1s 95.50946	

3d 1s 96.76073	3p 1s 99.17108	4s 1s 97.20182
3s 1s 102.5176	2s 1s 121.5023	2p 1s 111.2407
6s ² 2s 383.4423	6d 2s 387.7044	6p ² 2s 384.7807
7p 2s 387.9537	5p ² 2s 391.9551	5s ² 2s 388.8073
7s 2s 396.9075	5d 2s 398.658	6p 2s 397.11
4p ² 2s 403.9255	5p 2s 413.2329	6s 2s 410.0702
4d 2s 420.2975	4p 2s 446.4547	5s 2s 433.9367
3d 2s 475.1783	3p 2s 539.582	4s 2s 486.0092
6s ² 2p 540.9091	6d 2p 549.4294	6p ² 2p 543.5764
7p 2p 549.9302	5p ² 2p 558.0052	5s ² 2p 551.647
7s 2p 568.0965	5d 2p 571.6896	6p 2p 568.5116
4p ² 2p 582.5843	5p 2p 602.1456	6s 2p 595.4535
4d 2p 617.2642	3s 2s 656.1123	5s 2p 647.1366
4p 2p 675.3772	4s 2p 770.2026	3d 2p 743.3515
3p 2p 914.0169	6p ² 3s 930.4459	6s ² 3s 922.658
6d 3s 947.7274	5s ² 3s 954.3452	7p 3s 949.2184
5p ² 3s 973.5361	6p 3s 1005.971	7s 3s 1004.672
5d 3s 1015.964	6s 3s 1093.521	4p ² 3s 1050.889
5p 3s 1116.304	5s 3s 1281.469	4d 3s 1169.402
3s 2p 1307.336	6s ² 3p 1325.086	2p 2s 1317.15
6p ² 3p 1341.208	7p 3p 1380.565	6d 3p 1377.413
5s ² 3p 1391.437	5p ² 3p 1432.611	4p 3s 1397.156
7s 3p 1501.068	5d 3p 1526.416	6p 3p 1503.969
4p ² 3p 1606.637	3d 3s 1723.116	6s 3p 1708.466
5p 3p 1764.739		6s ² 4s 1816.926

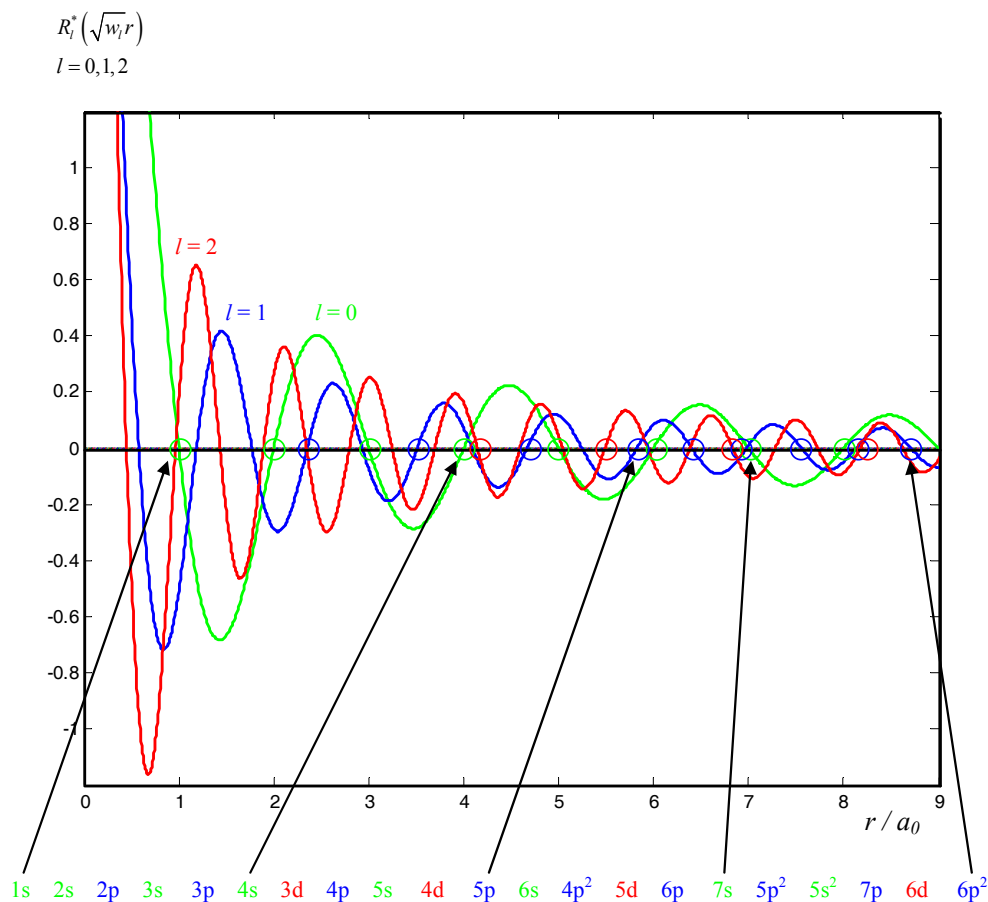


Figure 2. Sequence according to the increase in energy in the sub-shells filling up, in order to reproduce the Periodic Classification of the Elements

4. Conclusions

In this paper, we have considered the electron of Hydrogen as a three-dimensional e.m. spherical standing wave concentrically superimposed onto the e.m. standing wave of the proton. By hypothesizing a fractals form for the Hydrogen structure, it was possible to obtain a new periodic classification of the elements. Up till now, chemistry has considered atoms to be made up of sub-shells with 2, 6, 10, 14 electrons and, currently, the great number of electrons, 14, in sub-shells f creates some problems in the formation of the sixth and seventh periods. Instead, in this paper we considered only sub-shells with 2, 6, 10 electrons, to achieve a better ordering of the heavy metals. Then Ni, Pd, and Yb have been drawn up in columns in the new periodic classification of the elements. So it is possible to propose Ytterbium for the cold fusion experiments. Moreover, in accordance with Milan Perkovic's analysis (Perkovic, 2010), we obtained many fast decaying new theoretical e.m. wave-lengths of Hydrogen Spectrum. Do any appropriate tests exist for validating this? If so, the proposed approach to Hydrogen atomic structure (a superposition of the e.m. spherical standing waves of electron and proton) will have made a worthy experimental contribution. Furthermore, it is interesting to note that equations (7) are solutions of either the wave equation (1) (being applied to the Hydrogen atom) or the dynamic bi-Laplacian equation (Bellotti, 2009) that analyses the Hydrogen nuclear properties. Could this mathematical link be used in establishing a theory of cold fusion?

References

- Bellotti, G. (2009). The dynamic bi-Laplacian equation in polar coordinates and the magic numbers of atomic nucleus. *Phys. Essays*, 22(268). <http://dx.doi.org/10.4006/1.3141024>
- Bellotti, G. (2011). The hydrogen atomic model founded on the electromagnetic standing waves. *Phys. Essays*, 24(364). <http://dx.doi.org/10.4006/1.3601519>

- Jordan, E. C. (1985). *Reference Data for Engineers* (VII - 1988). Indianapolis, IN: Howard W. Sams & Company. 3.13-16.
- Perkovac, M. (2002). Quantization in Classical Electrodynamics. *Phys. Essays*, 15(41). <http://dx.doi.org/10.4006/1.3025509>
- Perkovac, M. (2003). Absorption and Emission of Radiation by an Atomic Oscillator. *Phys. Essays*, 16(162). <http://dx.doi.org/10.4006/1.3025572>
- Perkovac, M. (2010). Statistical test of Duane-Hunt's law and its comparison with an alternative law. Retrieved from arXiv:1010.6083v1
- Persico, E. (1939). *Fondamenti della Meccanica Atomica* (VI-1971). Bologna: Zanichelli. 216- 223.
- White, H. E. (1934). *Introduction to Atomic Spectra*. New York, NY: Mc Graw-Hill - Kōgakusha.